Electrical conductivity of aqueous solutions of aluminum salts

J. Vila,[1] E. Rilo,[1] L. Segade,[1] O. Cabeza,[1,*] and L. M. Varela[2]
[1]*Departamento de Física, Universidade da Coruña, Campus da Zapateira s/n, 15071 A Coruña, Spain*
[2]*Departamento de Física de la Materia Condensada, Universidade de Santiago de Compostela, Campus Sur, 15706 Santiago de Compostela, Spain*
(Received 20 August 2004; published 17 March 2005)

We present experimental measurements of the specific electrical conductivity (σ) in aqueous solutions of aluminum salts at different temperatures, covering all salt concentrations from saturation to infinite dilution. The salts employed were $AlCl_3$, $AlBr_3$, AlI_3, and $Al(NO_3)_3$, which present a 1:3 relationship between the electrical charges of anion and cation. In addition, we have measured the density in all ranges of concentrations of the four aqueous electrolyte solutions at 298.15 K. The measured densities show an almost linear behavior with concentration, and we have fitted it to a second order polynomial with very high degree of approximation. The measurement of the specific conductivity at constant temperature reveals the existence of maxima in the conductivity vs concentration curves at molar concentrations around 1.5*M* for the three halide solutions studied, and at approximately 2*M* for the nitrate. We present a theoretical foundation for the existence of these maxima, based on the classical Debye-Hückel-Onsager hydrodynamic mean-field framework for electrical transport and its high concentration extensions, and also a brief consideration of ionic frictional coefficients using mode-coupling theory. We also found that the calculated values of the equivalent conductance vary in an approximately linear way with the square root of the concentration at concentrations as high as those where the maximum of σ appears. Finally, and for completeness, we have measured the temperature dependence of the electrical conductivity at selected concentrations from 283 to 353 K, and performed a fit to an exponential equation of the Vogel-Fulcher-Tamman type. The values of the calculated temperatures of null mobility of the four salts are reported.

DOI: 10.1103/PhysRevE.71.031201 PACS number(s): 72.80.−r, 72.60.+g, 72.10.−d, 82.45.Gj

INTRODUCTION

The study of the electrical conductivity of electrolyte solutions has become again an important research matter. This is because, from the practical point of view, the recent discovery of many potential applications of ionic liquids (molten salts at ambient temperature) demands the knowledge of the electrical conductivity magnitude for many purposes, both for pure ionic liquids and for their aqueous solutions [1,2]. Many of the most interesting ionic liquids proposed for practical applications are based on Al salts, and so the study of the electrical behavior of these salts in aqueous solutions (and in general, of all electrolytes with a 1:3 relationship between anion and cation charges) is attracting increasing doses of attention. In parallel, theoretical studies of transport properties of electrolyte solutions (particularly of 1:3 and other types of highly asymmetric electrolytes) are the object of renewed interest.

After intense experimental work during the late 19th century, theoretical studies of the electrical conductivity of electrolyte solutions began with the work of Arrhenius, and they suffered a great impulse with the advent of the Debye-Hückel (DH) mean-field statistical equilibrium theory of primitive model (PM) electrolyte solutions [3]. Based on this equilibrium picture of electrolytes, Onsager and Fuoss [4] formulated a hydrodynamic theory of ionic transport in the first half of the last century [3–8]. This is one of the oldest problems in physical chemistry and has been widely treated in literature for both the static and the frequency-dependent regimes. In the classical Debye-Hückel-Onsager (DHO) theory [9], hydrodynamic equations of motion are combined with the DH equilibrium theory for calculating the transport coefficients of electrolyte solutions. This formalism is based on the assumptions that the ions undergo Brownian motion and that the DH equilibrium distribution functions are preserved under weak external fields. On the basis of these assumptions DHO formalism made important contributions to transport theory of electrolytes, particularly the celebrated Onsager limiting law of conductance that allowed the understanding of years of experimental research. DHO treatment was soon generalized by Debye and Falkenhagen [10] to account for the effect of high frequency fields on the conductance and dielectric constant of the fluid. In addition, Joos and Blumentritt [11] analyzed the effect of high intensity fields on electrolytic conductance, the so-called Wien effect.

The classical DHO theory was derived under mean-field conditions and for highly diluted solutions, so it is not expected to be accurate for finite concentrations. Many strategies have been developed to improve the DHO limiting predictions including ionic association and purely empirical results [5,6]. Transport properties are directly related to equilibrium properties of the solution, and the equilibrium distribution functions determine the dynamic behavior of the medium. Consequently, any improvement in the equilibrium distributions of the media must yield modifications in the related transport theory formalism. The old linear response DHO theory based on the extension of the DH equilibrium theory to transport phenomena has been recently improved

*FAX: +34 981 167065. Email address: oscabe@udc.es

using more accurate pair distribution functions. These include the mean-spherical approximation (MSA) for both the restricted primitive model [12,13] and the unrestricted primitive model (PM, different ionic sizes) [14–17]. These equilibrium theories are extensions of the hard core DH theory which satisfy the Stillinger-Lovett second moment condition [18] and have been shown to provide more accurate expressions for the thermodynamics and transport coefficients of electrolyte systems. However, to our knowledge, no maxima in the conductivity concentration curves are predicted in the concentration range analyzed in these schemes.

Recently, DHO transport formalism has been combined with the formally exact dressed-ion theory equilibrium structural model of the fluid [19–21] to derive transport equations, giving rise to the so called dressed-ion transport theory derived in the late 1990s by Varela *et al.* [22,23]. In this formalism, the ionic charges and screening length of the fluid are replaced by renormalized values at finite concentrations, and the latter are evaluated using a modified version of the MSA equilibrium structural model [21]. The renormalized charges act as kinetic agents in the transport process and this allows the extension of the mean-field predictions to fairly high concentrations (for an extensive review of formally exact mean-field theories of ionic fluids see Ref. [24] and references therein).

In recent years, attention has been focused again on finding new fully microscopic theoretical models of ionic microscopic dynamics applicable throughout all the concentration range using mode-coupling (MC) theory and density functional techniques [19]. However, these theories provide highly formal expressions that are mainly indicated for simple 1:1 electrolyte solution, so the development of a complete theoretical framework of electrolyte transport is still an open question.

In this paper we present the experimental measurement of the specific electrical conductivity and density in aqueous solutions of aluminum salts at 298.15 K and atmospheric pressure, covering all range of concentrations, from saturation to highly dilute solutions. We have measured both magnitudes for aqueous solutions of $AlCl_3$, $AlBr_3$, AlI_3, and $Al(NO_3)_3 \cdot 9H_2O$. Also, we have measured the temperature behavior of the conductivity for selected concentrations from 283 to 353 K. Let us note that, to our knowledge, in spite of the great amount of results on the electrical conductivity of aqueous solutions of electrolytic salts (see Refs. [5,6] and references therein, and [21–23] for particular studies on conductivity maxima of several salts), the results published here for the conductivity of aluminum salts with monovalent anions in the whole concentration regime up to saturation seem to have not been previously published. Moreover, we report here the calculated null mobility temperatures of aluminum halides and nitrate, at which the diffusivity of the solutions vanishes, indicating that the systems have lost their liquidlike (intensive) thermodynamic and flow properties, which is highly related to the occurrence of conductivity maxima.

THEORETICAL SECTION

The existence of maxima in the conductivity vs concentration curves is a general feature of normal electrolyte solutions, and has been widely reported in literature for both aqueous [25–27] and nonaqueous [28] solutions. Conductivity maxima have been reported even for ionic surfactant solutions in nonaqueous solvents [29]. The ability of electrolyte solutions to carry current would be expected to increase with the volume density of charge carriers in solutions. Nevertheless, it always peaks at high enough concentrations for aqueous solutions [2] due to the attenuation of the ionic mobility associated with the concentration-enhanced electrostatic interactions between the ions. Claes and co-workers [27] have pointed out the coincidence of the concentration of the conductivity maxima with the composition of the glass transition of electrolyte solutions, where the supercooled ionic solution splits into two immiscible phases [30,31]: a crystalline water-rich phase composed essentially of hydrogen-bonded pure water and a salt-rich vitreous phase formed by hydrated ions. The glass transition temperature is approximately 10 K higher than the null mobility temperature in the Vogel-Fulcher-Tamman (VFT) equation, commonly employed to describe transport properties in viscous fluids, and its behavior with ionic concentration varies depending on the region where the solution lies: for solutions whose concentration is higher than the concentration of the maximum of the conductivity-concentration curve, the glass transition temperature increases with concentration, and the opposite behavior is registered for solutions in the diluted regime. Angell [32] has related the appearance of the maxima in the conductivity-concentration curves to this breaking of the dependence of the glass transition temperature. According to this interpretation, the conductivity maximum would be indicative of the transition from a solution formed essentially by low-mobility hydrated ions to a hydrogen-bonded structured water regime in the bulk.

Despite much experimental evidence of conductivity maxima in aqueous electrolyte solutions, up to our knowledge, the only theoretical calculations reported in literature are those of Molénat [25], based on the conductivity definition and purely empirical evidence of electrolytic conductance behavior, and Angell [32], who used a relation between the equivalent conductance and concentration based on VFT theory. The phenomenological argument of Molénat rests completely on the monotonic decrease of ionic mobility vs concentration curves, and due to its simplicity and formal interest we shall briefly review it in this section.

The relation between conductivity and equivalent conductance is given by the well-known expression

$$\sigma = \Lambda c, \tag{1}$$

where c is the solute concentration expressed in equivalent moles per unit volume (i.e., the molar concentration divided by the chemical valence). Equation (1) is nothing but the definition of the equivalent conductance. Differentiating the above expression one obtains

$$d\sigma = c\, d\Lambda + \Lambda\, dc, \tag{2}$$

where the first term in Eq. (2) represents the effect of an increase of concentration on the ionic mobility, and the second term gives the effect of the charge density increase on the variation of the solution conductivity. Molénat employs

the experimentally observed decrease of $\Lambda(c)$ (equivalently, the decrease of ionic mobility) to justify the opposite sign of the terms of Eq. (2). At low concentrations, the charge density contribution of the first term of Eq. (2) dominates over the ionic mobility decrease, while at higher concentrations the decrease of ionic mobility predominates. This antagonistic behavior must lead to a cancellation of both effects at a definite concentration where both effects are equal in absolute value, identified by Molénat with the concentration of the conductivity maximum.

Molénat's argument, despite its formal power, is simple and completely qualitative, and its hypotheses must be clearly founded on theoretical grounds. Up to our knowledge, no quantitative results based on the classical DHO theory of electrolytic conductance or on more elaborate integral equations or molecular dynamical formalisms have been reported for conductivity maxima, and this is the main aim of the rest of this section.

When the ionic solution is perturbed by a homogeneous stationary electric field $\vec{E}$, the medium responds with the current density in the bulk,

$$\vec{j} = \sum_i n_i q_i \vec{v}_i = \sum_i n_i q_i \omega_i \vec{E}, \tag{3}$$

where the summation extends over all the species in solution. n_i, q_i, and ω_i are, respectively, the number density, the ionic charge, and the mobility of ions of species i. Using the microscopic Ohm's law one gets for the electrical specific conductivity

$$\sigma = \sum_i n_i q_i \omega_i. \tag{4}$$

The total mobility of an ion of species i is the result of its mobility in the infinite dilution limit, ω_i^0, where it only suffers interactions with the surrounding solvent molecules, as there are no other ions within a finite distance. The effect of the interionic interactions in solution, non-negligible at finite concentrations, is responsible for the introduction of concentration-dependent terms in the ionic mobility. The main consequences of the interaction between the electric charges of the ions are the electrophoretic effect and the relaxation effect [4–7]. The electrophoretic effect is due to the fact that the motion of an ion through a viscous medium distorts the velocity field around it as it tends to drag with it the solution in its vicinity and, therefore, the ions in its atmosphere do not move in a medium at rest. On the other hand, the relaxation effect is the result of the induction of a relaxation field by the distortion of the ionic atmosphere under the effect of the external field, and it is responsible for the relaxation of the system to equilibrium after the perturbation produced by the external force. Both phenomena are associated with the existence of long-ranged electrostatic interactions, and they reduce the mobility of the charged particles in the bulk fluid with respect to its limiting (ideal) value, so the macroscopic conductance of an ionic solution is expected to be a decreasing function of concentration.

Taking both phenomena into account, the total mobility of an ion of species i in solution is calculated in DHO formalism as [7]

$$\begin{aligned}\omega_i &= \omega_i^0 + \delta\omega_i^{electrof} + \delta\omega_i^{relax} \\ &= \omega_i^0 - \frac{k_D}{6\pi\eta} - \frac{\omega_i^0 |q_1 q_2|}{3\varepsilon k_B T} \frac{q^*}{1+\sqrt{q^*}} k_D.\end{aligned} \tag{5}$$

This result is generally referred to as the "limiting law for electrical conductance" [7] and its derivation was one of the great scientific achievements of its time. $k_B T$ is the thermal energy at absolute temperature T. On the other hand, ω_i^0 is the limiting mobility of ions of the species i, η is the viscosity, and ε is the dielectric constant of the solvent continuum (the classical theory rests on the primitive model of the solvent). k_D is Debye's screening parameter:

$$k_D^2 = \frac{4\pi}{\varepsilon k_B T} \sum_i n_i q_i^2. \tag{6}$$

The parameter k_D contains the effect of the whole medium (reflecting the mean-field character of the DH formalism); as it is proportional to $n^{1/2}$ (and so to $c^{1/2}$ it controls the spatial range of the effective mean-field potential created by ion i in the bulk [3]:

$$\overline{\psi_i}(r) = \frac{q_i}{4\pi\varepsilon r} e^{-k_D r}. \tag{7}$$

Finally, the parameter q^* in Eq. (5) is given by

$$q^* = \frac{(q_1\omega_1^0 - q_2\omega_2^0)}{(q_1 - q_2)(\omega_1^0 - \omega_2^0)}. \tag{8}$$

As follows from Eq. (5), the correction to the infinite dilution mobility of an ion in a bulk solution is proportional to Debye's parameter or equivalently to the square root of concentration. Substitution of Eq. (5) into Eq. (4) leads to the low concentration behavior of the specific conductivity:

$$\sigma = \sum_i n_i q_i \left[\omega_i^0 - \frac{k_D}{6\pi\eta} - \frac{\omega_i^0 |q_1 q_2|}{3\varepsilon k_B T} \frac{q^*}{1+\sqrt{q^*}} k_D \right]. \tag{9}$$

In this result, the expression inside the brackets is a linearly decreasing function of $c^{1/2}$, while the ionic number density of species i grows linearly with concentration. Therefore, in the infinite dilution regime—the range where DHO expression (5) is valid—the function $\sigma(c)$ increases with c, in agreement with experimental results (see, for example, the extensive collection of data contained in Refs. [5,6]), and confirming Molénat's argument in the highly dilute regime.

However, the approximations involved in the derivation of the limiting law for electrical conductance in Eq. (5) (see Refs. [5,6] for details) limit its range of validity to concentrations up to $C \approx 0.001$ eq mol l^{-1}, so it is obvious that the limiting form of this formalism cannot be used for considerations valid up to the maximum of conductivity in electrolyte solutions. Curiously, Eq. (9) qualitatively predicts the existence of a maximum in the $\sigma(c)$ curve, although one cannot reasonably expect it to be quantitatively accurate, due to the intrinsically limiting character of the DHO formalism.

In addition, all the previously mentioned results that extend the original DHO results to finite concentrations predict, with more or less precision, a decrease of the ionic equivalent conductance for solutions of concentrations up to 1.0*M*, reflecting a decrease of the ionic mobility with increasing number of charge carriers, therefore confirming Molénat's argument up to these concentrations.

The above results concerning Molénat's argument must be confirmed using a fully microscopic theory for conductance of ions at finite concentrations. A nonphenomenological framework of ionic dynamics based on the MC theory of friction is due to Chandra and Bagchi (see [33] and references therein). In this work, time-dependent density functional theory and the MCT formalism are used to obtain self-consistent expressions for the ionic cloud fluctuations arising from the interaction of the moving ion with the surrounding ions, and for the electrophoretic term originating from the coupling of the ion velocity to the collective current mode of the ion atmosphere. In this framework, the Laplace transform of the microscopic electrolyte friction is given by [33,34]

$$\frac{1}{\delta\varsigma_i(z)} = \frac{1}{\delta\varsigma_{i,rel}(z)} + \frac{1}{\delta\varsigma_{i,elect}(z)}, \tag{10}$$

where $\delta\varsigma_{i,rel}(z)$ is the contribution of the interactions of the central ion of species i with the surrounding ions, and $\delta\varsigma_{i,elect}(z)$ is a term of hydrodynamic origin due to the coupling of the tagged ion with the current velocity. Chandra and Bagchi obtained expressions of these friction coefficients using the mean-field self-consistent equilibrium structural model of electrolyte solutions due to Attard [18], and proved numerically that these coefficients are monotonically increasing functions of the ionic concentration in concentrated solutions, which implies a monotonic decrease of ionic mobility. This definitely confirms theoretically that maxima in conductivity-concentration curves must exist for electrolyte solutions at sufficiently high concentrations, although we still lack detailed quantitative expressions for the prediction of their actual values.

EXPERIMENTAL SECTION

The four chemicals used are all from Aldrich, and they present a purity better than a 98%, except for AlI_3, which it is better than 95%. The water used to prepare the solutions has a milli-*Q* grade. The electrical conductivity data σ we present here have been measured using a conductimeter from Crison, model GLP31. We have employed a measurement cell suitable for the measured conductivity value (with a cell constant of $C=1\ \mathrm{cm}^{-1}$, which has a resolution around 1%. This conductimeter uses an ac current of 4.5 V peak and 500 Hz frequency in the range of σ we measure. The use of an ac current and the fact that the electrodes are platinized allowed us to neglect the polarization effect in the electrodes [35]. Also, the capacitive effect that appears between the electrodes immersed in the conductivity liquid is minimized by the low frequency used, and so it can be ignored [35]. To regulate the temperature of the sample we use a Selecta thermostat, calibrated with an Anton Paar thermometer model DT 100-30, which has a resolution of 0.1 K in the range of temperatures used. All data presented here have been measured several times in different samples to ensure reproducibility within 10% in absolute value.

The measurement procedure has been described previously [36]. It was designed to obtain the maximum resolution and to avoid contamination of the samples. Before each measurement session the conductimeter is calibrated with two certified 0.01*M* and 0.1*M* KCl solution supplied by Crison. After the calibration, the measurement cell is washed with ethanol, and washed again later with a sample of the compound we are going to measure, we discard that sample and the measurement is performed with a new one. Finally, when the temperature of the sample is stable, we perform each single measurement as fast as possible (a few seconds) to minimize undesirable effects that would modify the measured values (such as self-heating of the samples, ionization in the electrodes, etc.) [35,37]. When measuring σ vs concentration dependence of the solution, we began with the saturated solution and dilute it adding selected quantities of milli-*Q* water to obtain the next concentration. In every step the sample is weighed to quantify tiny losses of mass and to correct concentration.

Densities of solutions were measured with an Anton-Paar DMA 60/602 vibrating tube densimeter, thermostated at $T=298.15\pm0.01$ K in a Haake F3 circulating-water bath. Immediately prior to each series of measurements, distilled water and heptane were used to calibrate the densimeter. Thus, we obtain an accuracy in the measured density better than 0.1 kg m^{-3}. Finally, all mixtures were prepared by mass using a Mettler AT 201 balance with an sensitivity of 10^{-3} g. The precision of the Al^{3+} concentration calculated is then estimated to be better than 10^{-3}.

It is interesting to note that the Al halide salts react with violence with the water, liberating to the atmosphere hydrogen halides. So the concentration is always referred to the Al^{3+} ion. Also, it is well known that the Al ion hydrolyzes in acid solutions, being thus in octahedral coordination with six water molecules, i.e., the $[Al(H_2O)_6]^{3+}$ ion, neutralized by the corresponding OH^- anions.

RESULTS AND DISCUSSION

As mentioned below, we measured the mass density (ρ) of all four solutions versus the Al^{3+} molar fraction (x) from infinite dilution up to saturation ($x\approx0.06$). The precision of the measurement was chosen to be 10^{-3} g cm^{-3}, and all the reported measurements were performed at a constant temperature of 298.15 K. In Fig. 1 we plot the obtained ρ vs x for the four solutions analyzed. In this figure (as in the rest of the figures presented in this paper), solid dots correspond to AlI_3, open dots to $AlBr_3$, solid squares to $AlCl_3$, and open squares to $Al(NO_3)_3$. The resulting data were fitted to a second order polynomial equation of the form

$$\rho = A_2x^2 + A_1x + A_0. \tag{11}$$

The obtained A_i coefficients are shown in Table I, together with the corresponding regression factor R^2. Let us note that A_0 corresponds to the density of milli-*Q* grade water used for

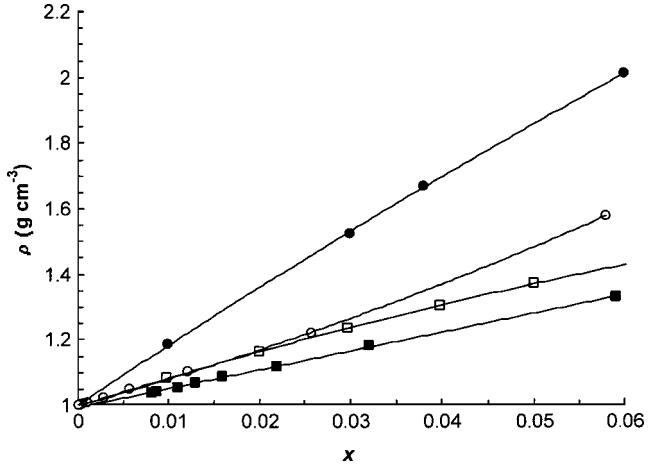

FIG. 1. Density (ρ) vs molar fraction of the Al^{3+} ion in the aqueous solution. Solid dots correspond to AlI_3, open dots to $AlBr_3$, solid squares to $AlCl_3$, and open squares to $Al(NO_3)_3$. The line is the best fit of Eq. (11) to the data points. The parameters used appear in Table I.

calibration, and so their value is the same for all solutions. In Fig. 1, the solid curves represent the best fit of Eq. (11) with the A_i fitting parameters given in Table I. As observed, all ρ vs x curves are almost linear, mainly for solutions of $AlCl_3$; one of them is concave (solutions of $AlBr_3$), while the other two are convex [solutions of AlI_3 and $Al(NO_3)_3$]. From a practical point of view, Eq. (11) allows us to calculate the concentration C of the Al^{3+} cations in equivalent moles per liter (eq mol l^{-1}) units knowing its molar fraction x. In the case of Al^{3+} the unit eq mol l^{-1} corresponds to the molarity divided by 3. This last can be easily calculated with high precision by weight measurements.

In Fig. 2 we present the measured concentration dependence of the specific electrical conductivity σ vs C for the four studied salts in all the range of concentration, up to saturation. As can be observed in that plot, there appears a peak in the four σ vs C curves at around the same value of $C \approx 4.5$ eq mol l^{-1}, except for $Al(NO_3)_3$ which presents its maximum at a slightly higher concentration $C \approx 6$ eq mol l^{-1}. As shown in Fig. 2 the concentration of the maximum is only slightly influenced by the size of the anion, which is reasonable if one takes into account the low hydration of the anionic species. In addition, the value of the conductivity at the maximum increases with the anion size [except again for $Al(NO_3)_3$ which presents the biggest anion size and the lowest σ value]. These results are in apparent

TABLE I. Coefficients A_i and regression factors R^2 from the fitting of the density ρ (g cm^{-3}) vs the molar fraction of Al^{3+} (x) to a second order polynomial given by Eq. (11).

	A_2	A_1	A_0	R^2
AlI_3	−30.3	18.7	0.9970	0.9999
$AlBr_3$	37.2	7.9	0.9970	0.9998
$AlCl_3$	4.0	5.5	0.9970	0.9991
$Al(NO_3)_3$	−28.4	8.9	0.9970	1.0000

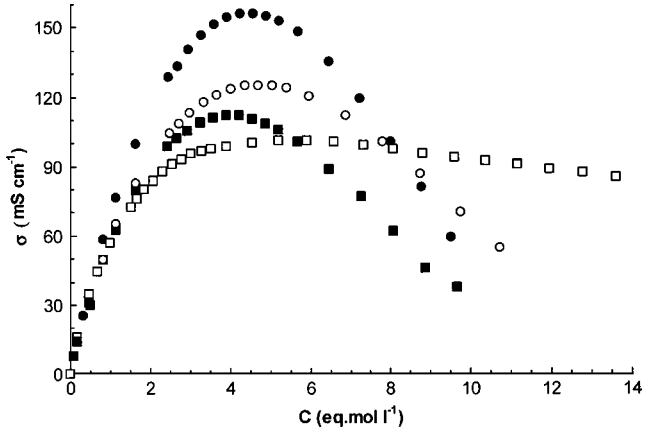

FIG. 2. Electrical conductivity (σ) vs concentration of the Al^{3+} ion in the aqueous solution (in eq mol per liter, i.e., the molarity divided by 3). Solid dots correspond to AlI_3, open dots to $AlBr_3$, solid squares to $AlCl_3$, and open squares to $Al(NO_3)_3$.

contradiction with the Nernst-Einstein equation

$$\Lambda_i = \frac{D_i q_i N_A}{k_B T}, \tag{12}$$

where N_A is Avogadro's number. The above result attributes a higher conductivity to species of higher diffusion coefficient D_i. The diffusion coefficient for spherical ions of radius r_i may be related to the solvent's viscosity η by the Stokes-Einstein equation

$$D_i = \frac{k_B T}{6\pi\eta r_i}. \tag{13}$$

Thus, one would expect that the salts with the bigger anions would show a lower conductivity, contrary to experimental evidence near the maxima. However, one should bear in mind that the Nernst-Einstein equation is valid only if no perturbation of the ionic fluxes by other ionic species exists, so, given the infinite range of the ionic interaction, the law is valid only for infinitely diluted ionic solutions, where the four solutions present a very similar conductivity. Thus, no contradiction exists, but one must explain the behavior of the curves in the vicinity of the specific conductivity peaks. This behavior can be understood if one considers that the hydration of the anionic species increases as the electronegativity increases, so the hydration of the chlorides is less negative than that of the iodides and bromides. Thus, the chlorides are expected to be less mobile than bromides or iodides at low but otherwise finite concentrations. Water molecules have higher mobilities in the neighborhood of Br^- or I^- than near Cl^- so viscosity forces opposing ionic diffusion are lower for the former ionic species.

It is also noteworthy that the above behavior is inverted in the vicinity of saturation, according to previous results reported by Molénat [25]. At saturation, the σ value of $Al(NO_3)_3$ is the highest, while the order between iodide and bromide is inverted with respect to that in the maxima. Chloride presents the lowest σ value until saturation, although it is apparent that its specific conductivity would also surpass

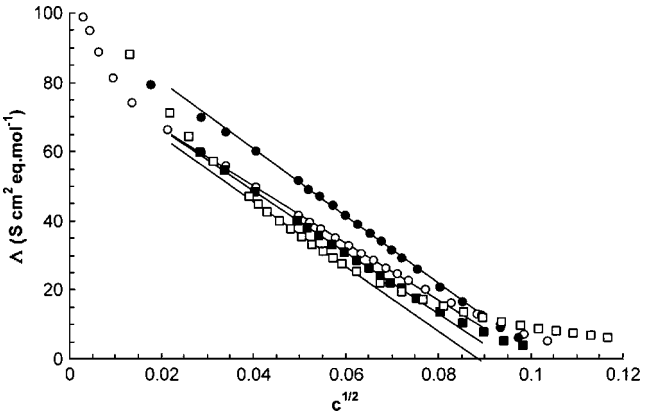

FIG. 3. Equivalent conductance (Λ) vs square root of the concentration of the Al^{3+} ion in the aqueous solution (in eq mol per cm^3, i.e., the molarity divided by 3000). Solid dots correspond to AlI_3, open dots to $AlBr_3$, solid squares to $AlCl_3$, and open squares to $Al(NO_3)_3$. The straight lines represents Eq. (14) with the parameters given in Table II. That equation was fitted to the data around the concentration where the peak in the conductivity appears. See text for details.

the values of the other halides at higher concentrations. At these concentrations, the spheres of influence of the ions are considerably interpenetrated, so the interionic interactions become predominant, reducing drastically the mobility of the ions, which are forced to remain in almost fixed equilibrium positions. Under these circumstances, the strongly negatively hydrated iodide anions are the less mobile, and the opposite behavior is expected for chlorides. On the other hand, a qualitative explanation for the conductivity at the saturation of nitrate comes from the fact that, while halide salts react violently with water (in a different manner for each of them), the nitrate does not. So the concentration of free anions in the aluminum nitrate solution is higher than that for the halide solutions, which even present lower total anion concentrations at saturation.

In Fig. 3 we present the equivalent conductance ($\Lambda = \sigma/C$) of the four solutions studied vs the square root of the Al^{3+} concentration expressed in equivalents per cm^3 ($c^{1/2}$), covering all range of concentrations measured. We observe an approximately linear behavior of Λ with the square root of concentration in the range of concentrations where maxima in σ appeared, which can be fitted by an equation of the form

$$\Lambda = K_1 - K_2 c^{1/2} \tag{14}$$

where K_i are positive constants. Surprisingly, this linear relationship is similar to that predicted by the conventional DHO model given by Eq. (9). As mentioned above, the DHO model is valid only for very low concentrations ($C < 10^{-3}$ eq mol l^{-1}), where we have not enough measurements to apply it. However, we observe in Fig. 3 that Λ vs $c^{1/2}$ for the four solutions is approximately linear for concentrations up to $C \approx 8$ eq mol l^{-1}, a range where the concentrations of the maxima in σ of our solutions are contained (see Fig. 2). The obtained values of the best fitting of Eq. (12) between $C=2$ and 8 eq mol l^{-1} for the three halide solutions, and between $C=1.6$ and 3.6 eq mol l^{-1} for the nitrate, are compiled in Table II. As expected, the values of K_1 obtained do not correspond with the corresponding equivalent conductance at infinite dilution, Λ_0, of the salts used [38], because that value would have to be obtained by fitting infinitely diluted solutions. It is noteworthy that the obtained values of K_1 and of K_2 are of the same order for the four solutions, and the quality of the linear fit is fine in all cases, according to the value of the regression factor R^2 for each fit (also included in Table II).

TABLE II. Coefficients K_i and regression factors R^2 from the fitting of the equivalent conductance Λ (S cm^2 eq mol^{-1}) vs square root of the Al^{3+} concentration expressed in equivalents per unit volume in cm^3 ($c^{1/2}$), to the linear expression given in Eq. (14).

	K_2	K_1	R^2
AlI_3	1001	101.7	0.9996
$AlBr_3$	757	78.9	0.9979
$AlCl_3$	837	81.1	0.9984
$Al(NO_3)_3$	937	83.0	0.9989

Finally, we analyzed the temperature dependence of σ for selected concentrations of the four solutions from 283 to 353 K. For this purpose, we measured σ for the most diluted solution of AlI_3 (that with $C=0.32$ eq mol l^{-1}), the saturated one of $Al(NO_3)_3$ ($C=13.6$ eq mol l^{-1}) and for the concentration where the conductivity maxima are registered for the solution of $AlBr_3$ ($C=4.37$ eq mol l^{-1}). For the $AlCl_3$ solution we have measured the temperature dependence of four solutions: the diluted one ($C=0.50$ eq mol l^{-1}), at a concentration that is half that where the peak in σ appears ($C=2.12$), that of the peak ($C=4.25$), and for the saturated solution ($C=9.67$). Note that C is obviously a temperature-dependent magnitude, and consequently, for reproducibility purposes, we outline that these values of C correspond to those measured at 298.15 K. In Fig. 4 we plot the measured σ vs T curves for the four aqueous solutions (in the case of $AlCl_3$ we plot only the saturated solution). Although the observed temperature behavior is nearly linear, a curvature appears. In Fig. 5 we show the Arrhenius plot of the calculated $\ln \sigma$ vs T^{-1}, where we observe that the temperature dependence of the conductivity does not obey the Arrhenius law, i.e., $\ln \sigma(T) \propto A/T$. The curvature of the presented curves must be accounted for using the VFT function [39]

$$\sigma(T) = Ae^{-BT_0/(T-T_0)}, \tag{15}$$

where A and B are fitting parameters and T_0 represents the temperature of null mobility, at which the diffusivity of the ions in the solution vanishes. All the temperature dependence is placed in the mobility term in the exponential. The obtained fit of the data points to Eq. (15) appears in Fig. 5 for the selected concentrations chosen for each solution. The values of the different coefficients of Eq. (15) obtained from the best fit of the data appears in Table III, where we included the standard deviation s of each fit. However, due to the particular form of the Einstein mobility relation $D \approx \sigma T$,

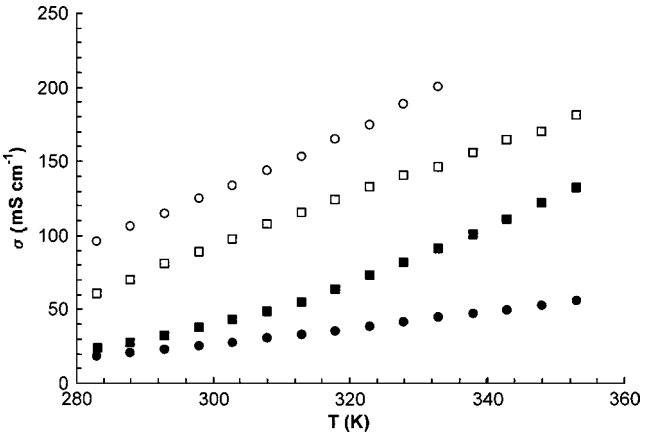

FIG. 4. Electrical conductivity (σ) vs temperature for selected concentrations. Solid dots correspond to AlI_3 ($C=0.32$), open dots to $AlBr_3$ ($C=4.73$), solid squares to $AlCl_3$ ($C=9.67$) and open squares to $Al(NO_3)_3$ ($C=13.6$). C is in units of eq mol per liter, i.e., the molarity divided by 3.

conductivity data are often fitted to the equation [39]

$$\sigma(T) = \frac{A'}{T} e^{-B' T_0'/(T-T_0')}. \tag{16}$$

Obviously, for high temperature data (those obtained for temperatures well above the null mobility temperature) the preexponential factor has a strong effect. The corresponding values of the positive constants A' and B' and the null mobility temperature T_0' for the systems under scrutiny in this paper obtained from the best fit of Eq. (16) to the measured data appear in Table IV, where we also include the corresponding standard deviation s, indicative of the quality of the fit. The value of T_0' is related to the temperature of the glass transition T_g at which the supercooled electrolyte solutions undergo a demixing into two phases, as we mentioned previously, losing their liquidlike thermodynamic and flow properties [31,39]. As observed in Tables III and IV, the values of T_0 and T_0' differ depending on the theoretical expression used, while both represent theoretically the same null mobility temperature. Also the fit is not very sensitive to the exact value of T_0 (or T_0') due to the fact that the temperature interval analyzed is not enough large.

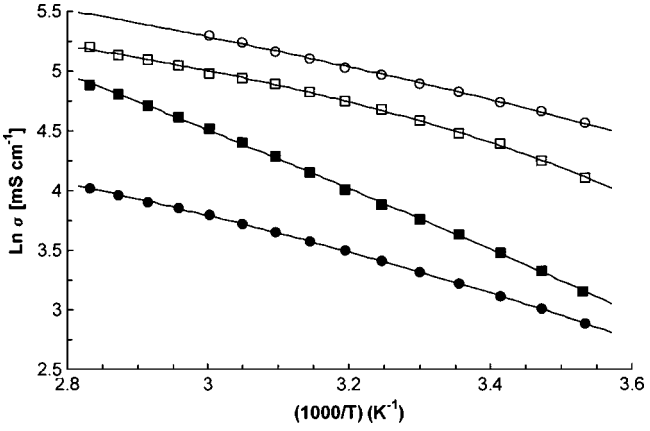

FIG. 5. Logarithm of the electrical conductivity ($\ln \sigma$) vs inverse of temperature for the same concentrations as in Fig. 4. Solid dots correspond to AlI_3, open dots to $AlBr_3$, solid squares to $AlCl_3$, and open squares to $Al(NO_3)_3$. The lines correspond to the best fit of Eq. (15) to the data points with the constant parameters given in Table III.

TABLE III. Coefficients A and B, and T_0, and regression factor s, from the fitting in a plot of the logarithm of conductivity $\ln[\sigma \text{mS cm}^{-1}]$ vs inverse of temperature $(T-T_0)^{-1}$ (K) to the regression given in Eq. (15).

C (eq mol l^{-1})	A	BT_0	T_0 (K)	s
AlI_3 ($C=0.32$)	365.8	351.4	166.8	0.004
$AlBr_3$ ($C=4.73$)	1354.9	353.9	149.6	0.010
$Al(NO_3)_3$ ($C=13.6$)	534.5	156.1	211.0	0.008
$AlCl_3$ ($C=0.50$)	17420.3	1290.1	87.9	0.012
$AlCl_3$ ($C=2.12$)	1000.0	687.25	96.7	0.012
$AlCl_3$ ($C=4.25$)	1586.4	553.5	107.6	0.007
$AlCl_3$ ($C=9.67$)	3636.0	678.2	149.4	0.022

CONCLUSIONS

In this paper we reported the experimental measurement of the electrical conductivity of aqueous solutions of four Al salts throughout all the range of concentrations up to saturation. Previously, we measured the density of all solutions at different Al^{3+} molar fractions and constant temperature of 298.15 K in order to express the concentration in conventional molar units. The corresponding curves for the density show different behavior for the different salts, one being nearly linear, another convex, and two others concave. The conductivity vs concentration curves show that all salts present maxima, around $C=4.5$ eq mol l^{-1} for the halide salts, and at about $C=6$ eq mol l^{-1} for the nitrate. We present the simple foundations of the classical Molénat argument based on the classical DHO theory and its extensions for high concentrations, definitely showing that there must exist a maximum in the conductivity-concentration profiles of electrolyte solutions, due to the compensation of the contri-

TABLE IV. Coefficients A' and B', and T_0', and regression factor s, from the fitting in a plot of the logarithm of conductivity $\ln[\sigma(\text{mS cm}^{-1})]$ vs inverse of temperature $(T-T_0)^{-1}$ (K^{-1}) to the regression given in Eq. (16).

C (eq mol l^{-1})	A' (units of 10^3)	$B'T_0'$	T_0' (K)	s
AlI_3 ($C=0.32$)	147.9	358.8	177.4	0.014
$AlBr_3$ ($C=4.73$)	205.4	150.1	212.3	0.019
$Al(NO_3)_3$ ($C=13.6$)	4714.8	1296.7	48.8	0.037
$AlCl_3$ ($C=0.50$)	159.7	347.9	172.7	0.021
$AlCl_3$ ($C=2.12$)	159.7	149.0	214.8	0.042
$AlCl_3$ ($C=4.25$)	205.4	145.5	223.1	0.045
$AlCl_3$ ($C=9.67$)	150.3	162.14	233.4	0.108

butions of ion concentration and interionic interactions. From the conductivity data we calculated the equivalent conductance, and found that Λ follows a linear relationship with the square root of the concentration in the concentration range near the conductivity peak, the corresponding slopes being very similar for all the substances under study. This behavior surprisingly coincides with that predicted by the classical mean-field limiting theories, while we observe here linear relationships for concentrations around 10^3 times higher than the upper limit of validity of the theoretical DHO model.

Finally, when we measure σ vs T we obtain a nearly linear relationship, which can be observed as a VFT exponential law if we fit the data to a given equation, which is proposed for the σ vs T relationship, and the temperatures of null mobility for aluminum halides and nitrate are obtained from high temperature conductivity data. As observed, the value of that temperature differs depending on the theoretical expression used to extract it. It would be the aim of a next paper to work on the best method to extract that temperature of null mobility, so interesting for the development of a quantitative theory about conductivity at high concentrations.

[1] T. Welton, Chem. Rev. (Washington, D.C.) **99**, 2071 (1999).
[2] W. Xu and C. A. Angell, Science **302**, 422 (2003).
[3] P. Debye and E. Hückel, Phys. Z. **24**, 185 (1923).
[4] L. Onsager and R. M. Fuoss, J. Phys. Chem. **36**, 2689 (1932).
[5] H. S. Harned and B. B. Owen, *The Physical Chemistry of Electrolyte Solutions*, 3rd ed. (Reinhold, New York, 1958).
[6] R. A. Robinson and R. H. Stokes, *Electrolyte Solutions* (Butterworths, London, 1959).
[7] J. B. Hubbard, in *The Physics and Chemistry of Aqueous Ionic Solutions*, edited by M. C. Bellisent-Funel, NATO Advanced Studies Institute, Series B: Physics (Reidel, Dordrecht, 1987), pp. 95–128.
[8] J. O'M. Bockris and A. K. N. Reddy, *Modern Electrochemistry* (Plenum, New York, 1998), Chap. 4.
[9] The DHO classical formalism for ionic conductance has also been referred to with various other names in the literature: Fuoss-Onsager formalism, Debye-Falkenhagen-Onsager formalism, etc., corresponding to different combinations of the names of the main researchers involved in its original derivation.
[10] P. Debye and H. Falkenhagen, Phys. Z. **29**, 121 (1928).
[11] G. Joos and M. Blumentritt, Phys. Z. **28**, 836 (1927).
[12] W. Ebeling and J. J. Rose, J. Solution Chem. **10**, 599 (1981).
[13] W. Ebeling and M. J. Grigo, J. Solution Chem. **11**, 151 (1982).
[14] O. Bernard, W. Kunz, P. Turq, and L. Blum, J. Phys. Chem. **96**, 3833 (1992).
[15] P. Turq, L. Blum, O. Bernard, and W. Kunz, J. Phys. Chem. **99**, 822 (1995).
[16] S. Durand-Vidal, J. P. Simonin, P. Turq, and O. Bernard, J. Phys. Chem. **99**, 6733 (1995).
[17] S. Durand-Vidal, P. Turq, O. Bernard, C. Treiner, and L. Blum, Physica A **231**, 123 (1996).
[18] P. Attard, Phys. Rev. E **48**, 3604 (1993).
[19] R. Kjellander and D. J. Mitchell, Chem. Phys. Lett. **200**, 76 (1992).
[20] R. Kjellander and D. J. Mitchell, J. Chem. Phys. **101**, 603 (1994).
[21] L. M. Varela, M. Pérez-Rodríguez, M. García, F. Sarmiento, and V. Mosquera, J. Chem. Phys. **109**, 1930 (1998).
[22] L. M. Varela, C. Rega, M. Pérez-Rodríguez, M. García, V. Mosquera, and F. Sarmiento, J. Chem. Phys. **110**, 4483 (1999).
[23] L. M. Varela, M. Pérez-Rodríguez, M. García, F. Sarmiento, and V. Mosquera, J. Chem. Phys. **111**, 10986 (1999).
[24] L. M. Varela, M. García, and V. Mosquera, Phys. Rep. **382**, 1 (2003).
[25] J. Molénat, J. Chim. Phys. Phys.-Chim. Biol. **66**, 825 (1969).
[26] R. C. Sharma, R. K. Jain, and H. C. Gaur, Electrochim. Acta **24**, 139 (1979).
[27] P. Claes, Y. Loix, and J. Glibert, Electrochim. Acta **28**, 421 (1983).
[28] G. Herlem, B. Fahys, M. Herlem, and J-F. Penneau, J. Solution Chem. **28**, 223 (1999).
[29] S. Dev, D. Das, and K. Ismail, J. Chem. Eng. Data **49**, 339 (2004).
[30] C. A. Angell and E. J. Sare, J. Chem. Phys. **49**, 4713 (1968).
[31] C. A. Angell and E. J. Sare, J. Chem. Phys. **52**, 1058 (1970).
[32] C. A. Angell, Aust. J. Chem. **23**, 929 (1970).
[33] A. Chandra and B. Bagchi, J. Chem. Phys. **110**, 10024 (1999).
[34] B. Bagchi, J. Chem. Phys. **109**, 3989 (1998).
[35] O. Klug and B. A. Lopatin, *New Developments in Conductimetric and Oscillometric Analysis* (Elsevier, Amsterdam, 1988).
[36] M. Prego, E. Rilo, E. Carballo, C. Franjo, E. Jiménez, and O. Cabeza, J. Mol. Liq. **102**, 83 (2003).
[37] J. Hamelin, T. K. Bose, and J. Thoen, Phys. Rev. A **42**, 4735 (1990).
[38] *CRC Handbook of Chemistry and Physics*, 80th ed. edited by David R. Lide (CRC, Boca Raton, FL, 1999).
[39] M. Videa, Wu Xu, B. Gell, R. Marzke, and C. A. Angell, J. Electrochem. Soc. **148**, 1352 (2001).